# Oxidative phosphorylation pathway disruption is an alternative pathological mechanism leading to Diamond-Blackfan anemia

Running head: OXPHOS disruption causes Diamond-Blackfan anemia

Rudan Xiao,[#1,2] Lijuan Zhang,[#1,2] Zijuan Xin,[#1,2] Junwei Zhu,[1] Qian Zhang,[1] Siyun Chu,[1] Jing Wu,[1,3] Lu Zhang,[1,2] Yang Wan,[4] Xiaojuan Chen,[4] Weiping Yuan,[4] Zhaojun Zhang,*[1,2,3,5,6] Xiaofan Zhu,*[4] and Xiangdong Fang*[1,2,3,5,6]

[1]Beijing Institute of Genomics & China National Center for Bioinformation, Beijing, P. R. China; [2]University of Chinese Academy of Sciences, Beijing, P. R. China; [3]Sino-Danish College, University of Chinese Academy of Sciences, Beijing, P. R. China; [4]State Key Laboratory of Experimental Hematology, Institute of Hematology and Blood Diseases Hospital, Chinese Academy of Medical Sciences & Peking Union Medical College, Tianjin, China; [5]Institute for Stem Cell and Regeneration, Chinese Academy of Sciences, Beijing, P. R. China; and [6]Beijing Key Laboratory of Genome and Precision Medicine Technologies, Beijing, P. R. China

[#]R.X., Lijuan Z., and Z.X. contributed equally to this study.

* Corresponding authors.

**Xiangdong Fang**

Beijing Institute of Genomics & China National Center for Bioinformation, Beijing 100101, P. R. China

Tel.: 86-010-84097495

Fax: 86-010-84097720

E-mail: fangxd@big.ac.cn

**Xiaofan Zhu**

State Key Laboratory of Experimental Hematology, Institute of Hematology and Blood Diseases Hospital, Chinese Academy of Medical Sciences & Peking Union Medical College, Tianjin 300020, China

Tel.: 86-022-23909001

Fax: 86-022-23909001

E-mail: xfzhu@ihcams.ac.cn

**Zhaojun Zhang**

Beijing Institute of Genomics & China National Center for Bioinformation, Beijing 100101, P. R. China

Tel.: 86-010-94087728

Fax: 86-010-84097720

E-mail: zhangzhaojun@big.ac.cn

Text word count: 4240 (introduction, results, discussion, methods not included that can be moved to supplemental materials)

Abstract word count: 215

Number of figures and tables: 6, 0

Number of references: 73

**Scientific Category:** red cells, iron, and erythropoiesis

**Key Points:**

- Oxidative phosphorylation (OXPHOS) pathway disruption is an alternative pathological mechanism underlying Diamond-Blackfan anemia (DBA).
- Suppression of OXPHOS leads to defects in erythropoiesis and ribosomal biogenesis via the RanGAP1 protein.

**Abstract**

Diamond-Blackfan anemia (DBA) is a rare congenital disorder characterized by the failure of erythroid progenitor differentiation; however, the molecular mechanisms leading to erythroid defects remain unclear. By analyzing the transcriptomic profiles of bone marrow from patients with DBA (n = 10), we identified the oxidative phosphorylation (OXPHOS) pathway as a possible cause of DBA. We established a DBA cell model using differentiating hematopoietic stem progenitor cells in which the OXPHOS pathway had been suppressed to completely recapitulate the defects of erythroid progenitor differentiation, ribosome biogenesis, and heme biosynthesis, which are representative characteristics of patients with DBA. Disruption of the OXPHOS pathway led to ribosomal defects and associated erythroid defects via the abolishment of RanGAP1, which is pivotal in the RNA transport pathway. The established DBA cells exhibited an overall reduction in ribosomal proteins, but not the composition of ribosomal proteins in the ribosome, which altered the translation of a subset of transcripts specific for erythropoiesis. We revealed that the OXPHOS pathway participates in erythropoiesis, particularly at an early stage, and the relationship between OXPHOS pathway and erythropoiesis was reinforced. CoQ10, an activator of OXPHOS, largely rescued the erythroid defects in DBA cells. Our results reveal that OXPHOS repression is an alternative pathological mechanism leading to DBA, demonstrating its potential as a therapeutic pathway in DBA.

## Introduction

Diamond-Blackfan anemia (DBA) is a rare inherited bone marrow failure syndrome characterized by erythropoiesis failure, leading to hypoplastic anemia, congenital defects, and a predisposition for malignancies [1]. Some patients present with occasional neutropenia or thrombocytosis [2]. However, DBA typically presents with erythroblastopenia caused by differentiation failure of the erythroid linage only. The molecular mechanisms underlying the DBA pathology remain unclear. Understanding the process of erythropoiesis and its underlying mechanisms may provide insights into the pathological mechanisms of DBA.

Mutations in numerous genes, including ribosomal and non-ribosomal proteins, have been identified as the causative agents of DBA [3, 4]. Most of these mutations lead to impaired ribosome biogenesis and erythroid defects at the progenitor cell stage because erythroid progenitor cells are sensitive to apoptosis caused by activation of the p53 pathway resulting from haploinsufficiency of ribosomal proteins in DBA [5]. Erythroid progenitor cells are also extremely sensitive to impaired translation, which may be attributable to the rapid cell division or high translational demand for globin synthesis in the erythroid cell lineage [5-7]. L-Leucine potently stimulates protein synthesis by activating mTOR signaling, which underlies the enhanced erythroid progenitor differentiation observed in DBA models [8, 9]. Heme biosynthesis facilitates globin production during erythropoiesis and proceeds with globin production in DBA cases, and decreased heme synthesis improves red blood cell production [10]. In addition to erythroid defects, impaired ribosome biosynthesis is a major feature of DBA pathology [11, 12], which can result in loss of the translation of a selected subset of transcripts specifically sensitive to erythropoiesis [7, 13], eventually leading to erythroid defects in DBA. Previously discovered pathological mechanisms underlying DBA are closely related to various aspects of erythropoiesis. We predicted that identifying the events involved in the regulation of early erythropoiesis can improve the understanding of DBA pathology, which may be useful for clinical research and applications.

Oxidative phosphorylation (OXPHOS) is highly dependent on proteins encoded by the mitochondrial genome and generates most of the energy required for cells through the mitochondrial electron transport chain [14-16]. OXPHOS is required for cell lineage specification and development [17] and is responsible for providing energy for differentiating hematopoietic stem progenitor cells (HSPCs) towards the erythroid lineage [18] but

not for the other lineages [19]. OXPHOS deficiency is among the most common genetically inherited diseases and can result in various diseases, with an estimated prevalence of related disorders of 1:5000 in humans [14]. However, the association between the OXPHOS pathway and erythropoiesis or related diseases is largely unknown.

Our study aims to clarify the role of OXPHOS pathway in erythropoiesis and further disclose the pathological mechanism involving this pathway underlying DBA, which may improve the understanding of erythropoiesis and provide more insights into the pathology of DBA.

## Materials and Methods

### Clinical samples

Bone marrow (BM) samples from patients with DBA (n = 10) and patients with idiopathic thrombocytopenic purpura (ITP; n = 3), who were included as the healthy control group [20], were obtained from Tianjin Blood Disease Hospital, Chinese Academy of Medical Sciences & Peking Union Medical College. DBA was clinically diagnosed according to established criteria [21, 22]. The age for the patients with DBA ranges from 4 to 120 months, and the mean age is 25.2 months. All patients with DBA included in the study had been diagnosed based on the procedures [23]. Three patients had mutations in RP (Ribosomal proteins) or physical deformities, including DBA-5 (*RPL11* mutation, limb deformities), DBA-9 (*RPS19* mutation), and DBA-10 (*RPL5* mutation, finger deformities) (Supplemental Table 1). Human cord blood samples from full-term newborns were obtained from Beijing Obstetrics and Gynecology Hospital, Capital Medical University (Beijing, China). The subjects provided written informed consent and the study was performed in accordance with the Declaration of Helsinki. The protocols for sample collection and use were approved by the ethics committee of the Beijing Institute of Genomics, Chinese Academy of Sciences.

### CD34+ cells

We isolated CD34+ cells from human cord blood and BM using an EasySep™ Human CD34 Positive Selection Kit II (STEMCELL Technologies, Vancouver, Canada); a sample purity of >95% was confirmed

using flow cytometry. When an expansion phase was required, CD34+ cells were cultured in StemSpan SFEM II medium (STEMCELL Technologies) supplemented with 50 μg/mL stem cell factor, 50 μg/mL Flt3 ligand (PeproTech, Rocky Hill, NJ, USA), 50 μg/mL Thrombopoietin) (PeproTech), and 1% penicillin and streptomycin solution for 6 days prior to differentiation. CD34+ cell purity was >95% after expansion, as determined using fluorescence-activated cell sorting. Erythroid cells were differentiated as described previously [24] with incubation at 37℃ and 5% $CO_2$.

## DBA cell model

Differentiating HSPCs with suppression of the OXPHOS pathway towards the erythroid lineage were used as the primary cell model to explore the relationship between OXPHOS and the DBA pathology. HSPCs were isolated from human cord blood or healthy BM from patients with ITP. Rotenone (Rot, R817233, Sigma-Aldrich, St. Louis, MO, USA), which inhibits the transfer of electrons from the iron-sulfur center to ubiquinone by interfering with the ability of NADH to produce ATP, was added at different concentrations (0, 0.5, and 1 μM) to the culture medium when erythroid differentiation was initiated from CD34+ cells. The extent of OXPHOS inhibition was measured using flow cytometry at different time points (24, 48, and 72 h) at the optimized concentration of Rot (1 μM). CoQ10 (C111044, Sigma-Aldrich), which activates OXPHOS by transporting electrons to the electron transport chain during respiration, was used to rescue the inhibitory effect of Rot on OXPHOS. CoQ10 (25 and 50 μM) was added to the culture medium for an additional 72 h after Rot treatment, and the difference between with and without CoQ10 treatment in cell membrane potential was measured using flow cytometry analysis.

### Colony-forming unit assay

Colony-forming unit assay was performed as previously described [24].

### Flow cytometry

To detect OXPHOS inhibition, Rot treated cells were collected and centrifuged at 300 ×$g$ for 10 min, and the pellet was resuspended in 70 μL Hanks' buffer. 20 μL of this cell suspension was retained without

staining as the blank control. When a change in mitochondrial membrane potential was detected, 10 μM rhodamine 123 fluorescent dye (R8004, Sigma-Aldrich) was added to the 50 μL cell suspension and incubated at 37°C for 30 min in the dark. The cells were washed twice with Hanks' buffer, and flow cytometry was performed. The level of OXPHOS inhibition was proportional to the ratio of the left peak count to the total count. To detect cell surface markers of the differentiated cells, flow cytometry was performed as per the previous study[24]. Flourescence-activated cell sorting analysis was conducted using a BD Biosciences Canto II flow cytometer (BD Biosciences, Franklin Lakes, NJ, USA). Data were analyzed using FlowJo 10.0.7 software (TreeStar, Ashland, OR, USA).

**Immunofluorescence assay**

On day 7, $10^5$–$10^7$ differentiated cells were collected into 2 mL centrifuge tubes, gently mixed with 2 mL of Dulbecco's phosphate-buffered saline (DPBS), and centrifuged at 1000 ×*g* for 5 min. After washing the cell pellet twice with DPBS, 4% paraformaldehyde was immediately added to fix the cells for 10 min, followed by centrifugation at 1000 ×*g* for 5 min. The pellet was washed thrice with DPBS, 0.4% Triton-X-100 was added to penetrate the cells for 15 min, and the cells were centrifuged at 1000 ×*g* for 5 min. The pellet was washed with DPBS thrice, and 5% bovine serum albumin-DPBS was added. After centrifugation at 1000 ×*g* for 5 min, primary antibodies against RPS6 (ab80158, Abcam, Cambridge, UK) and RPS3 (ab128995, Abcam) were separately added to the pelleted cells, which were allowed to stand at 25°C for 2 h. After washing with DPBS thrice, the fluorescently labeled goat anti-rabbit secondary antibody was added, incubated at room temperature for 1 h, and washed thrice with DPBS. The cells were evenly spread and dried on clean glass slides. DAPI and anti-fluorescence quencher coverslips were mounted and photographed using an upright fluorescence microscope (LSM710, Zeiss, Germany).

**knockdown of RanGAP1**

The plasmids and the procedures used for knocking down of RanGAP1 were as per the previous study [24]. Primer sequences used for knockdown were shown in Supplemental Table 2.

**Real-time PCR**

The procedures for total RNA extraction and real-time PCR were followed as previously described [25]. Primers used for quantitative PCR were listed in Supplemental Table 2.

**Western blotting**

Cells were lysed with RIPA buffer (50 mM Tris-HCl at pH 7.4, 150 mM NaCl, 0.1% SDS, 1% NP-40, 0.25% sodium deoxycholate, 1 mM dithiothreitol) supplemented with protease inhibitors (Roche, Basel, Switzerland) and incubated for 30 min on ice. After centrifugation at 18,800 × g for 10 min, the supernatant concentration was determined. Equal amounts of protein were separated using sodium dodecyl sulfate (SDS)-polyacrylamide gel electrophoresis in Tris/glycine/SDS running buffer. The proteins were transferred onto a polyvinylidene fluoride membrane in Tris/glycine transfer buffer. The membranes were blocked with 3% bovine serum albumin-TBST (Tris Buffered Saline with Tween 20) for 1 h at room temperature and then probed with the primary RanGAP1 mouse monoclonal antibody (ab92360, Abcam) at a 1:500 dilution and HBG2 (ab137096, Abcam), GATA1 (ab181544, Abcam), β-actin mouse monoclonal antibodies (HC201-01, TransGen Biotech, Beijing, China) at a 1:1000 dilution in 3% bovine serum albumin-TBST at 4℃ overnight. Membranes were rinsed with TBST thrice for 10 min each and incubated with secondary antibody for 1 h at room temperature. The membrane was rinsed with TBST solution thrice and placed in an Image Quant ECL machine (Tanon 5200, Tanon, Shanghai, China) for exposure photography.

**RNA-sequencing**

Total RNA was harvested from different samples using TRIzol reagent for RNA-sequencing (RNA-Seq) library construction. BM samples were lysed to remove red blood cells, and mononuclear cells were isolated using a Ficoll density gradient, followed by total RNA isolation. Total RNA was isolated from differentiated cells on days 3 and 7, and each group consisted of two biological replicates. RNA-Seq libraries were sequenced on an Illumina sequencing platform (San Diego, CA, USA), generating pair-end with 150 bp raw data. At least 4G of data were collected for further analysis. We used FastQC software for quality control, and the original sequence fastq file was compared to the UCSC version hg38 reference file using HISAT2 software. The gene expression matrix file obtained using StringTie software was used as the input file to analyze

differentially expressed genes (DEGs). We used the R package edgeR for differential expression gene analysis with a biological coefficient of variation of 0.1. The DEG screening criteria were |log fold-change (FC)| > 1 and $p < 0.05$. The DEGs were utilized for bioinformatics analysis, including with Kyoto Encyclopedia of Genes and Genomes, Gene Ontology, and Gene Set Enrichment Analysis (GSEA).

**Single-cell transcriptome sequencing data analysis**

The single-cell RNA-seq data were downloaded from the Gene Expression Omnibus database (GSE139369 and GSE150774). A total of 49,707 single-cell transcriptome data was collected, including 12,602 BM mononuclear cells, 8,176 CD34+-enriched BM mononuclear cells, 14,804 peripheral blood mononuclear cells, and 14,125 terminal erythroid cells (CD34-CD235a+) isolated directly from the adult BM. These data were generated using 10 × Genomics 3 single-cell RNA sequencing. Gene expression was standardized using the default parameters of R package Seurat (version 4.0.6). Principal component analysis (dims = 20) was performed to reduce the dimensions of the data. UMAP was performed to visualize individual cells. We annotated the cells using the R package SingleR (version 1.8.0) and published datasets [26, 27]. Cells at different stages of HSC differentiation into red blood cells were selected, and hallmark gene sets were downloaded from the GSEA database. GSEA was performed using the R package GSVA (version 1.14.1) to determine the OXPHOS gene set enrichment scores in erythroid cells at different stages of differentiation.

**Proteome analysis**

Differentiated cells on day 7 were used for mass spectrometry (MS) and RNA-Seq analyses. Each group consisted of three biological replicates. The manipulations including protein extraction, trypsin digestion, tandem mass tag (TMT) labeling of peptides and LC-MS/MS analysis were referred to the previous description [28]. We separately researched the resulting spectra against the database using Proteome Discoverer 2.2 (PD 2.2, Thermo Fisher Scientific). The mass tolerance of the precursor ion was 10 ppm and mass tolerance of the product ion was 0.02 Da. No more than two miscleavage sites were allowed. The identified protein contained at least unique peptide with a false discovery rate (FDR) of ≤ 1.0%. Reporter quantification (TMT 10-plex) was used for TMT quantification. Significantly differentially expressed proteins between the experimental

and control groups were screened as the following criterion: $p < 0.05$ and $|\log2FC| > 0$. Gene Ontology and Kyoto Encyclopedia of Genes and Genomes analyses were performed using ClusterProfiler (version 4.0.2).

### Data availability

The supporting datasets of RNA-Seq for DBA samples and differentiated cells are respectively available from the Genome Sequence Archive with accession number HRA002012 and HRA002000. The following links were respectively created to allow a review of the records: https://ngdc.cncb.ac.cn/gsa-human/. The supporting datasets of proteomic data of this study is available from the Genome Sequence Archive with accession number OMIX971, and the following links was created to allow a review of the record: https://ngdc.cncb.ac.cn/omix/.

### Statistical analysis

Data was represented as mean ± standard deviation (SD). Statistical analyses were performed using GraphPad Prism (version 8.0.2) and $P < 0.05$ was considered statistically significant. Student's t-test was used: $*p < 0.05$; $**p < 0.01$; $***p < 0.001$.

## Results

### Disruption of OXPHOS may cause DBA

To explore the pathogenesis of human DBA from a broad perspective, we subjected the BM samples of the DBA and control groups to bulk transcriptome sequencing. The clinical characteristics of the DBA cohort are shown in Supplemental Table 1. Transcriptomic analysis revealed that abnormally disturbed genes in DBA were significantly enriched in the OXPHOS pathway ($p = 2.51E-41$), mitochondrial dysfunction ($p = 1.99E-41$), mTOR pathway ($p = 6.76E-5$), and heme biosynthesis II ($p = 1.10E-4$) (Figure 1A). The OXPHOS pathway is highly dependent on the proteins encoded by the mitochondrial genome, which has not been reported in DBA. Analysis of the transcriptome profiles of DBA samples against the control showed that OXPHOS was inhibited in 7 of 10 DBA cases, including the case with *RPL11* mutation, and the clustering of these DBA cases closely resembled the pattern observed for all genes in the OXPHOS pathway (Figure 1B),

suggesting that OXPHOS is involved in the pathogenesis of DBA. The ribosome biogenesis pathway was also significantly inhibited in DBA cases (Figure 1C). GSEA showed that these two suppressed pathways were enriched in DBA samples compared to in controls (Figure 1D). The transcriptome profiles of OXPHOS and the ribosome pathway in DBA were highly positively correlated up to 0.96 (Figure 1E), indicating that OXPHOS and ribosome biogenesis may utilize a mutual regulatory mechanism in DBA. As DBA is a ribosomopathy [29, 30], suppression of the OXPHOS pathway may be an alternative pathogenic pathway of DBA.

Further, to explore the association of the OXPHOS pathway with erythropoiesis, we analyzed single-cell transcriptome data using the BM of healthy individuals and profiled cells differentiated towards the erythroid lineage under normal physiological conditions (Figure 1F). We found that the OXPHOS pathway is finely controlled throughout erythropoiesis, exhibiting the highest activity at the pro-erythroblast stage, which is thought to demand higher energy for the stage transition from burst-forming unit-erythroid (BFU-E) / colony-forming unit-erythroid (CFU-E) to the early stage of terminal erythroid differentiation, suggesting that suppression of the OXPHOS pathway blocks erythroid differentiation at the progenitor cell stage (Figure 1G). We also identified other interesting pathways regulating erythropoiesis, such as heme biosynthesis which is specifically active throughout terminal erythroid differentiation and is initiated at the pro-erythroblast stage; these results are consistent with the pathology of DBA [10].

**Suppression of OXPHOS leads to failure of erythroid progenitor differentiation**

The development of HSPCs into erythroid cells can serve as a cell model for exploring the pathogenesis of hematological disorders associated with mitochondrial dysregulation [19]. We developed an *ex vivo* culture system to differentiate human HSPCs into erythroid cells, in which the OXPHOS pathway is inhibited by Rot [31], a specific inhibitor of the OXPHOS pathway. A greater reduction in the mitochondrial membrane potential (P3) indicates greater suppression of the OXPHOS pathway [32]. We found that addition of Rot inhibited OXPHOS in dose- and time-dependent manners (Figure 2A, B) and decreased ATP production in the treated cells (data not shown). Thus, we developed a cell model of DBA cells in which the OXPHOS pathway was suppressed.

Blocked differentiation at the BFU-E or CFU-E stages is a hallmark of DBA [10, 33]; if suppression of OXPHOS causes of DBA, erythropoiesis failure is also expected to occur. To evaluate this hypothesis, we conducted a CFU assay with CD34+ cells as the starting cells in which the OXPHOS pathway was inhibited. DBA cells with OXPHOS inhibition generated normal numbers of myeloid cells but significantly reduced the colony numbers of BFU-E, CFU-E, and CFU-GEMM, which include erythroid lineage cells, indicating specific loss of erythroid progenitors (Figure 2C). This indicates that erythropoiesis occurs was impaired at the same stage as in patients with DBA. Flow cytometry assay showed that inhibition of OXPHOS led to a visible decrease in differentiated CD71+GlyA+ erythroid cells (3.57%), which was caused by obvious blockage at the stage of erythroid progenitors derived from both BM and cord blood sources (Figure 2D–F). Additionally, erythroid progenitors (CD71+ GlyA-) showed a decreasing trend beginning on day 3 in both models (Supplemental Figure 1 A-B). Decreased globin expression is characteristic of DBA phenotypes [10]. Globin expression showed a differential pattern in differentiated erythroid cells with or without Rot treatment on day 7, with dramatically reduced expression of *HBB* and *HBG*; *HBG* showed the highest expression among the globins (Figure 2G), indicating that erythroid defects in DBA cells occur at the early stage of erythroblasts or before entering the pro-erythroblast stage. Reduced globin expression in DBA cells may result from disruption of heme production [10], and we revealed that most genes involved in heme biosynthesis, particularly, *ALAS2*, that is the initial and rate-limiting gene of heme biosynthesis, gradually decreased in DBA cells during erythroid differentiation (Figure 2H, Supplementary Figure 1C), suggested that disruption of the heme biosynthesis pathway is caused by suppression of OXPHOS in DBA cells. Erythroid-specific genes, mostly transcription factors, were decreased in DBA cells (Figure 2I, Supplementary Figure 1D), among which GATA1 is a DBA-causing non-RP gene [7, 34, 35]. These results demonstrate that inhibition of OXPHOS suppression of these erythroid-specific factors reflects the failure of erythropoiesis in DBA cells. Moreover, we observed increased apoptosis and expression of apoptosis marker genes during erythroid differentiation (Supplementary Figure 1E–F), which are typical features of DBA cells [13].

**Suppression of OXPHOS leads to defects in ribosome biogenesis pathway**

Ribosomal abnormalities can result from defects in DBA-causative genes [13, 36] or the reduced abundance of ribosomal proteins [11]. Further, we evaluated whether alterations in ribosomal protein genes occurred in

our DBA cells with suppressed OXPHOS pathways in differentiating HSPCs undergoing commitment to the erythroid lineage. We comprehensively characterized the transcriptomic features of the DBA cells on days 3 and 7, which mainly represent erythroid progenitors and further differentiated erythroid cells during HSPCs undergoing commitment to the erythroid lineage [26, 27] (Figure 3A). Significantly suppressed DEGs in DBA cells on days 3 and 7 were enriched in the OXPHOS pathway and ribosome biogenesis pathway, which are disturbed in patients with DBA (Figure 3B), suggesting that disruption of the ribosome pathway resulted from the suppression of OXPHOS. Ribosomal genes most relevant to DBA, including RPL and RPS, were significantly suppressed ($p < 0.001$) in the Rot-treated group compared to in the control on day 3 (Supplemental Figure 2A) and day 7 (Figure 3C). We also observed disturbed RNA transport and spliceosome pathways in DBA cells (Figure 3B).

Ribosomal markers are proteins specific to ribosomes and facilitate recognition of ribosome morphology and integrity. The immunofluorescence assay revealed that DBA cells had significantly lower expression of RPS3 and RPS6 than control cells, which are non-DBA causative proteins and specific markers of ribosomes [35] (Figure 3D–E, Supplemental Figure 2B–C). These results suggest that the ribosome morphology was disrupted in our DBA cells with the suppressed OXPHOS pathway and support that OXPHOS is disrupted and ribosome biogenesis is defective in patients with DBA. Therefore, suppression of OXPHOS led to a decreased abundance of ribosomal proteins in our DBA cells.

**OXPHOS suppression causes ribosomal defects via RanGAP1**

The RNA transport pathway was disturbed in DBA cells ($p < 1.00E-6$) (Figure 3B), indicating that an RNA transport defect can occur with the onset of OXPHOS suppression. The ribosome largely consists of rRNA; to explore the mechanism by which OXPHOS suppression leads to ribosome abnormalities in DBA cells, the transcriptomic data were mapped to the hsa03013-RNA transport pathway [37]. The results revealed the suppression of RAN (Ran GTPase) (Figure 4A), which is bound to GTP in the nucleus and GDP in the cytoplasm and is essential for the translocation of RNA and proteins through the nuclear pore complex [38]. RanGAP1 (Ran GTPase-activating protein 1), a RAN interacting protein, associates with the nuclear pore complex, and participates in regulating nuclear transport [39]. RanGAP1 plays an important role in regulation

of the RanGTP/GDP cycle [40]. We predicted that Ran-dependent nuclear transport, specifically the Ran cycle, was disrupted, which may have disturbed the expression of the GTPase–activating protein of the Ran cycle, RanGAP1. The Rot-treated group showed abolishment of RanGAP1 (Figure 4B), whereas the SUMO1/RanGAP1 complex that is involved in mitotic spindle formation but not in nuclear transport during interphase was only slightly suppressed [41]. Taken together, suppression of OXPHOS in DBA cells may lead to defects in the ribosome via RanGAP1, thereby disrupting the Ran cycle and blocking rRNA transport.

Hypothesizing that RanGAP1 is a downstream target of OXPHOS suppression and leads to ribosomal defects, it may participate in regulating erythropoiesis. To test this hypothesis, we designed independent shRNAs targeting different regions of RanGAP1 (Figure 4C) and observed consistent erythroid defects in various assays. Suppression of RanGAP1 in HSPCs almost abolished HBG expression (Figure 4D) and delayed erythroid differentiation (Figure 4E), resulting in defects in erythroid differentiation, as demonstrated by the reduced number of CD71+GlyA+ double-positive cells on day 7 (Figure 1F). These defective phenotypes in erythroid differentiation persisted until day 14 (Supplemental Figure 3A–E), although the expression of RanGAP1 recovered. Decreased expression of the representative DBA causative genes *RPL5* and *RPS19* may represent ribosomal defects resulting from the effects of RanGAP1 (Supplementary Figure 3F). Overall, suppression of the OXPHOS pathway may lead to ribosomal defects and associated defects in erythropoiesis via RanGAP1.

**Overall reduction in abundance of RPs and erythroid defects in DBA cells**

As ribosomal defects were observed under suppressed OXPHOS in DBA cells, we further examined the alterations of ribosomal proteins and effects of reduced ribosome levels on the translation of mRNAs to proteins in DBA cells. Therefore, we performed TMT-based quantitative proteomics in parallel with transcriptome sequencing in DBA cells (Figure 5A) and observed perturbations of RPs in the ribosomes at both mRNA and protein levels (Figure 5B). In proteomic analysis, all 80 RPs were detectable by two or more unique peptides, and the estimated protein abundance was robust across biological replicates (data not shown). Ribosomal defects in DBA cells were detected as decreased expression of all ribosomal proteins (Figure 5B), whereas the composition was unchanged. In accordance with the finding that DBA can result from reduced

ribosome abundance but not from changes in the ribosome composition [11], we observed significant alterations of over 90% DBA causative RPs that lead to erythroid defects in our DBA cells.

The high-throughput data for representative proteins or genes revealed reproducible decreases in the expression of erythroid-associated markers (e.g., GYPA, CD71, TF), transcription factors (e.g., GATA1, KLF1, LMO2), and globin (e.g., HBG1, HBB, HBA2) at both the transcriptome and proteome levels (Figure 5C). Interestingly, we also observed significant suppression of the heme biosynthesis pathway in DBA cells (Figure 5C), confirming that heme biosynthesis is disrupted by inhibition of OXPHOS during the differentiation of HSPCs into erythroid cells [10, 42]. Analysis of the functions of simultaneously differentiated expressed proteins and genes revealed disturbances in $O_2/CO_2$ exchange and apoptosis in DBA cells (Figure 5D), indicating an abnormality in erythropoiesis [43]. Our integrative omics data support that defects in ribosomes and erythropoiesis occurred in DBA cells.

mRNAs are typically vulnerable to fluctuations in ribosome concentrations, and thus certain cell types (e.g., erythroid cells) that depend on the protein levels of these mRNAs are sensitive to perturbations in the ribosome concentration [11, 44]. A reduction in the abundance of ribosomal proteins leads to decreased translation of a subset of proteins that are sensitive to erythropoiesis [7, 13, 45]. Therefore, we comprehensively screened genes without changes in transcript expression but showing a significant decrease in protein expression after translation. We identified inefficiently translated genes that may be sensitive to ribosomal defects in our DBA cells (Figure 5E). FAM122A is the most significantly downregulated protein in DBA cells (Figure 5E) that is abnormally upregulated in patients with β-thalassemia [46]. Downregulation of FAM122A can lead to reduced GATA1 transcriptional activity by decreasing its association with the target DNA in erythroid cells during terminal erythroid differentiation [46]. We identified a subset of sensitive genes whose functions have not been characterized in erythropoiesis to ribosome defects, except for *HBG1* and *FOXJ2* [47]. These sensitive and downregulated proteins were enriched in the pathways of RNA splicing and transport, translational initiation and protein targeting to the ER, and ribonucleoprotein complex biogenesis (Figure 5F). These disturbed pathways may be associated with DBA pathology by reducing the translation of their related transcripts under the abnormal regulation of ribosomal subunits or specific ribosomal proteins.

**CoQ10 rescues erythroid defects in DBA cells**

To verify whether OXPHOS inhibition causes erythroid defects, the OXPHOS activator CoQ10 was used to treat DBA cells. Following addition of CoQ10, the inhibitory effects of Rot on OXPHOS were significantly alleviated in DBA cells, as revealed by the increase in mitochondrial membrane potential (Figure 6A) and significant increase in ATP production compared to in cells treated with Rot ($p < 0.001$) (Figure 6B). Further, we tested the effect of CoQ10 on the expression of RanGAP1, which participates in erythropoiesis and was almost abolished by inhibition of OXPHOS in DBA cells. Interestingly, the suppression effect was completely rescued by addition of $CoQ_{10}$ by reversing the inhibition of OXPHOS (Figure 6C), whereas expression of the SUMO1/GAP1 complex was not suppressed [41]. To verify whether these defects were directly caused by OXPHOS inhibition, a $CoQ_{10}$ rescue experiment was performed. Flow cytometry analysis revealed that a visible decrease in differentiated GlyA+CD71+ double-positive erythroid cells (1.17%) was alleviated up to 23.4% by addition of $CoQ_{10}$ (Figure 6D), suggesting that CoQ10 restores early erythroid defects in DBA cells because erythropoiesis in patients with DBA cannot progress past the proerythroblast stage [48, 49]. We also observed phenotypic changes in OXPHOS suppression in differentiated HSPCs following Giemsa staining (Figure 6E), revealing a reduced number of proerythroblasts and delayed erythroid differentiation in DBA cells, which was partially alleviated by addition of CoQ10.

## Discussion

The molecular mechanisms fundamental to the pathogenesis of DBA are not completely understood. We characterized the regulation of OXPHOS in erythropoiesis and explored the molecular mechanism of this pathway in the regulation of DBA pathology. We first revealed that the OXPHOS pathway is an alternative mechanism regulating DBA pathogenesis and is disturbed in many patients with DBA with or without RP mutations. The OXPHOS pathway was not disturbed in established zebrafish DBA models with RP gene mutations [50-53], suggesting that OXPHOS is not the downstream pathway of DBA RP causative agents, but that an alternative pathogenic pathway exists in patients with DBA.

Several pathways are associated with the pathology of DBA. Ribosomal protein haploinsufficiency is the primary cause of DBA. Non-ribosomal proteins, including GATA1,TSR2, EPO, and CECR1, have also been shown to play an essential role in the pathogenesis of DBA in recent years [3, 4]. In the presence of certain RP abnormalities, the identified pathways including activated p53, mTOR, heme biosynthesis, and autophagy are associated with the pathology of DBA [4, 5, 10, 54-56]. Dysfunction of mitochondrial metabolism also seriously impacts erythroid differentiation. For example, loss of mitochondrial ATPase inhibitor 1 can cause severe anemia, and defects in this protein may contribute to human congenital sideroblastic anemia and other mitochondrial dysfunction-related diseases [57]. As the main energy supply system of mitochondria, OXPHOS dysfunction is crucial in the occurrence of mitochondrial diseases. Our established DBA cells with suppression of OXPHOS recapitulated most aspects of DBA defects, including erythroid progenitor differentiation, ribosome biogenesis, and heme biosynthesis, which are representative features of DBA. A molecular mechanism accounting for all aspects of DBA has not been determined. All mechanisms involved in DBA, including OXPHOS, are interconnected, at least partially, and none are mutually exclusive.

Disruption of the OXPHOS pathway can destroy ribosome biogenesis via the RNA transport pathway and lead to erythroid defects. There are two types of RNA nuclear transport, Ran-independent and Ran-dependent transport. The former is mainly mediated by the transcription–export complex, with NXF1 as the export receptor and binding poly(A)+ RNA [58], which are mostly mRNAs [59]. Whereas Ran-dependent export is mostly for rRNA or ribosomal subunits; thus, disruption of Ran-dependent export affects ribosome biogenesis [ 60, 61]. We observed that inhibition of OXPHOS led to suppressed Ran GAP1 expression, likely affecting the Ran-dependent RNA export mechanism and resulting in rRNA transport inhibition and defects in ribosome biogenesis. We examined DBA from a new perspective and the effect of OXPHOS inhibition on the Ran cycle in HSPCs differentiating into erythroid cells. We revealed a possible connection between OXPHOS inhibition and ribosomal suppression during erythroid differentiation, providing insight into the pathophysiology of DBA.

We examined why disruption of OXPHOS specifically leads to impaired erythropoiesis. A previous study revealed that mitochondrial biogenesis, including oxidative phosphorylation and ATP biosynthesis, was significantly affected during the differentiation of HSPCs into erythroid-specific pro-erythroblasts [19]. In

zebrafish, manipulation of the electron transport chain in the mitochondria is linked to erythropoiesis [31]. The OXPHOS pathway may be conserved in some species and is directly involved in erythropoiesis. In terms of energy consumption during erythroid differentiation, HSCs maintain their functions, such as division dynamics, mainly via the glycolysis pathway, and HSCs predominantly use aerobic glycolysis for ATP production rather than using OXPHOS [18, 62-65], whereas the OXPHOS pathway provides energy for erythroid lineage specification and erythroid differentiation [18, 66]. A surge of energy is required to initiate the erythroid differentiation of HSCs, during which glycolysis and OXPHOS can occur simultaneously, accompanied by a metabolic switch from glycolysis to OXPHOS, which is a driving force of erythroid differentiation [32]. OXPHOS provides energy for differentiating HSPCs towards the erythroid lineage, but not for other lineages [19], and the initiation of DBA pathology may occur because of disorder in energy usage switching during the differentiation of HSPCs into the erythroid lineage. The causes of anemia in patients with DBA are not well-understood. Our results suggest that the disrupted OXPHOS pathway can lead to erythroid defects in patients with DBA, likely by interfering with energy switching during erythroid differentiation. These results demonstrate the potential for curing erythroid defects in DBA disease from the perspective of energy intervention.

Mitochondrial respiration can drive the commitment of the erythroid lineage at an early stage [31]. Our data showed that erythroid defects occurred at an early stage of erythroid differentiation, likely because HSCs that undergo metabolic reprogramming exit the quiescent state and enter the active state in response to the increased energy demand for differentiating from erythroid progenitors to Pro-E. From the single-cell data in BM, we observed that the OXPHOS pathway was preferentially active at the early stage of pro-E but not at the stage of erythroid progenitors, suggesting that this pathway defect can occur between HSPCs and pro-E, consistent with observations in patients with DBA [13], resulting in blockage at the early stage of erythroid differentiation, and the cells cannot differentiate past the progenitor stage when this pathway was disrupted.

Heme biosynthesis is among the pathological mechanisms of DBA [10, 67]. Both suppressed OXPHOS and heme biosynthesis pathways have been detected in patients with DBA. One possible explanation for the defective heme biosynthesis in DBA cells is the interference of the interaction between heme and ribosomes that has limited availability in DBA cells caused by suppressed OXPHOS [68].

In DBA, certain RP mutations, including *RPL11*, *RPL5*, and *RPS19*, lead to ribosomal stress, which activates p53 and induces apoptosis [69]. The apoptotic cells were observed in established DBA cells. In DBA with certain RP mutations, erythroid progenitors or precursors are very sensitive to apoptosis caused by activation of p53 [49, 70], and defective erythroid phenotypes can be rescued by reducing the expression of p53 [52, 71]. We identified a subset of apoptosis-related proteins and genes; however, p53 was not detected in the proteomic data. Apoptotic cells may be produced via defective ribosome biogenesis because of their specific roles of ribosomal proteins in determining the erythroid lineage differentiation of HSPCs [13].

Previously, a single RP gene linked to ribosome biogenesis was extensively characterized [3, 12, 13]; however, the global defects in ribosome biogenesis that contribute to DBA pathology are largely unknown. In this study, we revealed that suppression of the OXPHOS pathway in differentiating HSPCs leads to dysfunction of ribosomal biosynthesis, as demonstrated by the overall reduction in the expression of ribosomal proteins, which may lead to abnormal translation of a selected erythroid-specific gene required for erythropoiesis [13, 44, 45]. Our results confirmed the relationship between the overall reduction of ribosomal proteins and defects in erythropoiesis.

New drugs or treatments have been needed for the patients with DBA. Small-molecule compounds that stimulate erythropoiesis are a class of drugs with great potential for treating DBA. By enhancing the specific upregulation of ribosome biosynthesis and protein translation through the mTOR pathway, L-leucine supplementation may dramatically improve anemia associated with ribosomal protein loss of DBA in mouse and zebrafish models [8, 9, 72]. SMER28, a small-molecule inducer of the autophagy pathway that regulates erythropoiesis, was also identified as a potential therapeutic drug for DBA [54]. A DYRK inhibitor that interferes with the p53 pathway in erythroid progenitors was screened as a potential drug in a doxycycline-inducible mouse model for RPS19-deficient DBA [73]. Our results suggest that activation of the OXPHOS pathway can be targeted to improve erythroid defects in patients with DBA. Additionally, OXPHOS defects may occur because of insufficient electron transfer from complexes I and II to complex III of the electronic transport chain, through which CoQ10, a small chemical molecule, largely alleviates erythroid defects at the base of disruption of the electronic transport chain, indicating its potential as a therapeutic drug for DBA. Thus, the OXPHOS pathway is a target of interest for DBA drug screening.

We observed the inhibited OXPHOS in 7 of 10 DBA cases that were not enough in numbers, which may be the first limitation of this study. The second limitation is that we studied the pathogenesis of DBA with the in vitro cell model throughout the study. Thus, the establishment of the in vivo association of OXPHOS inhibition with erythroid defects is needed, and it can be further explored in higher resolution at single cell level under BM microenvironment of DBA. Moreover, the reason why OXPHOS pathway is disrupted in some DBA BM is still a mystery. We proposed that it can be caused by the disorders in metabolic switch and alternative splicing events involving this pathway during HSCs differentiating into erythroid lineage under abnormal conditions in BM.

In summary, we examined the relationship between the OXPHOS pathway and erythropoiesis and discovered that disruption of OXPHOS may cause DBA. The disruption of OXPHOS is an alternative pathway of DBA pathogenesis and recapitulates the features in patients with DBA. We determined the molecular mechanism by which OXPHOS leads to DBA and reinforced the relationship between OXPHOS and ribosomal biogenesis in DBA. This study improves the understanding of erythropoiesis and provides insights into the pathology of DBA, which may improve translational research and applications for this disease.

## Acknowledgements

This research was supported by the Strategic Priority Research Program of the Chinese Academy of Sciences (grant no. XDA16010602), National Natural Science Foundation of China (Grant Nos. 81870097, 82070114, and 81700116), and National Key Research and Development Program of China (Grant Nos. 2017YFC0907400, 2016YFC0901700, 2018YFC0910700, and 2017YFC0907403).

## Author contributions

XF, XZ, and ZZ conceived and supervised the study; RX, LZ, ZX, and QZ analyzed the data; ZZ and RX designed the experiments; RX, LZ, JZ, LZ, and JW performed the experiments; ZZ, RX, and SC drafted the manuscript; XC and YW helped with sample collection. XF, XZ, ZZ, and WY revised the manuscript. All authors have read and approved the final manuscript.

## Conflict of interest

The authors declare there are not any competing financial interests in this study.

## References


1. van Dooijeweert, B., et al., *Pediatric Diamond-Blackfan anemia in the Netherlands: An overview of clinical characteristics and underlying molecular defects.* European Journal of Haematology, 2018. **100**(2): p. 163-170.
2. Willig, T.N., H. Gazda, and C.A. Sieff, *Diamond-Blackfan anemia.* Current Opinion in Hematology, 2000. **7**(2): p. 85-94.
3. Ulirsch, J.C., et al., *The Genetic Landscape of Diamond-Blackfan Anemia.* Am J Hum Genet, 2018. **103**(6): p. 930-947.
4. Da Costa, L., T. Leblanc, and N. Mohandas, *Diamond-Blackfan anemia.* Blood, 2020. **136**(11): p. 1262-1273.
5. Dutt, S., et al., *Haploinsufficiency for ribosomal protein genes causes selective activation of p53 in human erythroid progenitor cells.* Blood, 2011. **117**(9): p. 2567-2576.
6. Yip, B.H., et al., *Effects of L-leucine in 5q-syndrome and other RPS14-deficient erythroblasts.* Leukemia, 2012. **26**(9): p. 2154-2158.
7. Ludwig, L.S., et al., *Altered translation of GATA1 in Diamond-Blackfan anemia.* Nat Med, 2014. **20**(7): p. 748-53.
8. Jaako, P., et al., *Dietary L-leucine improves the anemia in a mouse model for Diamond-Blackfan anemia.* Blood, 2012. **120**(11): p. 2225-2228.
9. Payne, E.M., et al., *L-leucine improves the anemia and developmental defects associated with Diamond-Blackfan anemia and del(5q) MDS by activating the mTOR pathway.* Blood, 2012. **120**(11): p. 2214-2224.
10. Yang, Z.T., et al., *Delayed globin synthesis leads to excess heme and the macrocytic anemia of Diamond Blackfan anemia and del(5q) myelodysplastic syndrome.* Science Translational Medicine, 2016. **8**(338).
11. Mills, E.W. and R. Green, *Ribosomopathies: There's strength in numbers.* Science, 2017. **358**(6363).
12. Devlin, E.E., et al., *A transgenic mouse model demonstrates a dominant negative effect of a point mutation in the RPS19 gene associated with Diamond-Blackfan anemia.* Blood, 2010. **116**(15): p. 2826-2835.
13. Khajuria, R.K., et al., *Ribosome Levels Selectively Regulate Translation and Lineage Commitment in Human Hematopoiesis.* Cell, 2018. **173**(1): p. 90-+.
14. Torraco, A., et al., *Mouse models of oxidative phosphorylation defects: Powerful tools to study the pathobiology of mitochondrial diseases.* Biochimica Et Biophysica Acta-Molecular Cell Research, 2009. **1793**(1): p. 171-180.
15. Steele, S.L., S.V. Prykhozhij, and J.N. Berman, *Zebrafish as a model system for mitochondrial biology and diseases.* Translational Research, 2014. **163**(2): p. 79-98.
16. Chen, M.L., et al., *Erythroid dysplasia, megaloblastic anemia, and impaired lymphopoiesis arising from mitochondrial dysfunction.* Blood, 2009. **114**(19): p. 4045-4053.
17. Cliff, T.S. and S. Dalton, *Metabolic switching and cell fate decisions: implications for pluripotency, reprogramming and development.* Current Opinion in Genetics & Development, 2017. **46**: p. 44-49.
18. Oburoglu, L., et al., *Metabolic regulation of hematopoietic stem cell commitment and erythroid differentiation.* Current Opinion in Hematology, 2016. **23**(3): p. 198-205.

19. Liu, X., et al., *Regulation of mitochondrial biogenesis in erythropoiesis by mTORC1-mediated protein translation.* Nature Cell Biology, 2017. **19**(6): p. 626-+.
20. Guo, Y., et al., *Transfer RNA detection by small RNA deep sequencing and disease association with myelodysplastic syndromes.* Bmc Genomics, 2015. **16**.
21. Vlachos, A., et al., *Diagnosing and treating Diamond Blackfan anaemia: results of an international clinical consensus conference.* British Journal of Haematology, 2008. **142**(6): p. 859-876.
22. Boria, I., et al., *The Ribosomal Basis of Diamond-Blackfan Anemia: Mutation and Database Update.* Human Mutation, 2010. **31**(12): p. 1269-1279.
23. Vlachos, A. and E. Muir, *How I treat Diamond-Blackfan anemia.* Blood, 2010. **116**(19): p. 3715-3723.
24. Ren, Y., et al., *Regulatory association of long noncoding RNAs and chromatin accessibility facilitates erythroid differentiation.* Blood Adv, 2021.
25. Xin, Z.J., et al., *Mapping Human Pluripotent Stem Cell-derived Erythroid Differentiation by Single-cell Transcriptome Analysis.* Genomics Proteomics & Bioinformatics, 2021. **19**(3): p. 358-376.
26. Hu, J.P., et al., *Isolation and functional characterization of human erythroblasts at distinct stages: implications for understanding of normal and disordered erythropoiesis in vivo.* Blood, 2013. **121**(16): p. 3246-3253.
27. Li, J., et al., *Isolation and transcriptome analyses of human erythroid progenitors: BFU-E and CFU-E.* Blood, 2014. **124**(24): p. 3636-3645.
28. Wen, Y.Y., et al., *Quantitative proteomic analysis of scleras in guinea pig exposed to wavelength defocus.* Journal of Proteomics, 2021. **243**.
29. Narla, A. and B.L. Ebert, *Ribosomopathies: human disorders of ribosome dysfunction.* Blood, 2010. **115**(16): p. 3196-3205.
30. Narla, A., S.N. Hurst, and B.L. Ebert, *Ribosome defects in disorders of erythropoiesis.* International Journal of Hematology, 2011. **93**(2): p. 144-149.
31. Rossmann, M.P., et al., *Cell-specific transcriptional control of mitochondrial metabolism by TIF1 gamma drives erythropoiesis.* Science, 2021. **372**(6543): p. 716-+.
32. Richard, A., et al., *Erythroid differentiation displays a peak of energy consumption concomitant with glycolytic metabolism rearrangements.* Plos One, 2019. **14**(9).
33. Dianzani, I., E. Garelli, and U. Ramenghi, *Diamond-Blackfan anemia: A congenital defect in erythropoiesis.* Haematologica, 1996. **81**(6): p. 560-572.
34. Sankaran, V.G., et al., *Exome sequencing identifies GATA1 mutations resulting in Diamond-Blackfan anemia.* Journal of Clinical Investigation, 2012. **122**(7): p. 2439-2443.
35. Chennupati, V., et al., *Ribonuclease inhibitor 1 regulates erythropoiesis by controlling GATA1 translation.* J Clin Invest, 2018. **128**(4): p. 1597-1614.
36. Choesmel, V., et al., *Impaired ribosome biogenesis in Diamond-Blackfan anemia.* Blood, 2007. **109**(3): p. 1275-1283.
37. Rodriguez, M.S., C. Dargemont, and F. Stutz, *Nuclear export of RNA.* Biol Cell, 2004. **96**(8): p. 639-55.
38. Dahlberg, J.E. and E. Lund, *Functions of the GTPase Ran in RNA export from the nucleus.* Curr Opin Cell Biol, 1998. **10**(3): p. 400-8.
39. Ritterhoff, T., et al., *The RanBP2/RanGAP1(star)SUMO1/Ubc9 SUMO E3 ligase is a disassembly machine for Crm1-dependent nuclear export complexes.* Nature Communications, 2016. **7**.
40. Bischoff, F.R., et al., *Rangap1 Induced Gtpase Activity of Nuclear Ras-Related Ran.* Proceedings of the National Academy of Sciences of the United States of America, 1994. **91**(7): p. 2587-2591.
41. Joseph, J., et al., *SUMO-1 targets RanGAP1 to kinetochores and mitotic spindles.* J Cell Biol, 2002. **156**(4): p. 595-602.

42. Mercurio, S., et al., *The heme exporter Flvcr1 regulates expansion and differentiation of committed erythroid progenitors by controlling intracellular heme accumulation.* Haematologica, 2015. **100**(6): p. 720-729.
43. Testa, U., *Apoptotic mechanisms in the control of erythropoiesis.* Leukemia, 2004. **18**(7): p. 1176-1199.
44. Li, D. and J.L. Wang, *Ribosome heterogeneity in stem cells and development.* Journal of Cell Biology, 2020. **219**(6).
45. Flygare, J. and S. Karlsson, *Diarnond-blackfan anemia: erythropoiesis lost in translation.* Blood, 2007. **109**(8): p. 3152-3160.
46. Chen, J., et al., *FAM122A Inhibits Erythroid Differentiation through GATA1.* Stem Cell Reports, 2020. **15**(3): p. 721-734.
47. Yang, G.H., et al., *MicroRNAs Are Involved in Erythroid Differentiation Control.* Journal of Cellular Biochemistry, 2009. **107**(3): p. 548-556.
48. Sieff, C.A., et al., *Pathogenesis of the erythroid failure in Diamond Blackfan anaemia.* British Journal of Haematology, 2010. **148**(4): p. 611-622.
49. Ohene-Abuakwa, Y., et al., *Two-phase culture in Diamond Blackfan anemia: localization of erythroid defect.* Blood, 2005. **105**(2): p. 838-846.
50. Wan, Y., et al., *Transcriptome analysis reveals a ribosome constituents disorder involved in the RPL5 downregulated zebrafish model of Diamond-Blackfan anemia.* Bmc Medical Genomics, 2016. **9**.
51. Zhang, Z.J., et al., *Assessment of hematopoietic failure due to Rpl11 deficiency in a zebrafish model of Diamond-Blackfan anemia by deep sequencing.* Bmc Genomics, 2013. **14**.
52. Jia, Q., et al., *Transcriptome Analysis of the Zebrafish Model of Diamond-Blackfan Anemia from RPS19 Deficiency via p53-Dependent and -Independent Pathways.* Plos One, 2013. **8**(8).
53. Song, B.F., et al., *Systematic transcriptome analysis of the zebrafish model of diamond-blackfan anemia induced by RPS24 deficiency.* Bmc Genomics, 2014. **15**.
54. Doulatov, S., et al., *Drug discovery for Diamond-Blackfan anemia using reprogrammed hematopoietic progenitors.* Science Translational Medicine, 2017. **9**(376).
55. Heijnen, H.F., et al., *Ribosomal Protein Mutations Induce Autophagy through S6 Kinase Inhibition of the Insulin Pathway.* Plos Genetics, 2014. **10**(5).
56. Narla, A., et al., *L-Leucine improves the anaemia in models of Diamond Blackfan anaemia and the 5q-syndrome in a TP53-independent way.* British Journal of Haematology, 2014. **167**(4): p. 524-528.
57. Shah, D.I., et al., *Mitochondrial Atpif1 regulates haem synthesis in developing erythroblasts.* Nature, 2012. **491**(7425): p. 608-12.
58. Viphakone, N., et al., *TREX exposes the RNA-binding domain of Nxf1 to enable mRNA export.* Nature Communications, 2012. **3**.
59. Slomovic, S., et al., *Polyadenylation of ribosomal RNA in human cells.* Nucleic Acids Research, 2006. **34**(10): p. 2966-2975.
60. **Harvey Lodish, A.B., Chris A. Kaiser**, *Molecular Cell Biology*, in *Molecular Cell Biology*. 2016, W. H. Freeman: New York. p. 626.
61. Johnson, A.W., E. Lund, and J. Dahlberg, *Nuclear export of ribosomal subunits.* Trends in Biochemical Sciences, 2002. **27**(11): p. 580-585.
62. Du, W., et al., *SCO2 Mediates Oxidative Stress-Induced Glycolysis to Oxidative Phosphorylation Switch in Hematopoietic Stem Cells.* Stem Cells, 2016. **34**(4): p. 960-971.
63. Simsek, T., et al., *The Distinct Metabolic Profile of Hematopoietic Stem Cells Reflects Their Location in a Hypoxic Niche.* Cell Stem Cell, 2010. **7**(3): p. 380-390.
64. Takubo, K., et al., *Regulation of Glycolysis by Pdk Functions as a Metabolic Checkpoint for Cell Cycle Quiescence in Hematopoietic Stem Cells.* Cell Stem Cell, 2013. **12**(1): p. 49-61.
65. Baumann, K., *Stem cells: A metabolic switch.* Nat Rev Mol Cell Biol, 2013. **14**(2): p. 64-5.

66. Cabon, L., et al., *AIF loss deregulates hematopoiesis and reveals different adaptive metabolic responses in bone marrow cells and thymocytes.* Cell Death and Differentiation, 2018. **25**(5): p. 983-1001.
67. Mercurio, S., et al., *Alteration of heme metabolism in a cellular model of Diamond-Blackfan anemia.* European Journal of Haematology, 2016. **96**(4): p. 367-374.
68. Chiabrando, D. and E. Tolosano, *Diamond Blackfan Anemia at the Crossroad between Ribosome Biogenesis and Heme Metabolism.* Adv Hematol, 2014. **2010**(8): p.: 790632.
69. Lipton, J.M. and S.R. Ellis, *Diamond-Blackfan anemia: diagnosis, treatment, and molecular pathogenesis.* Hematol Oncol Clin North Am, 2009. **23**(2): p. 261-82.
70. Tsai, P.H., S. Arkin, and J.M. Lipton, *An intrinsic progenitor defect in Diamond-Blackfan anaemia.* Br J Haematol, 1989. **73**(1): p. 112-20.
71. Ellis, S.R., *Nucleolar stress in Diamond Blackfan anemia pathophysiology.* Biochim Biophys Acta, 2014. **1842**(6): p. 765-8.
72. Stipanuk, M.H., *Leucine and protein synthesis: mTOR and beyond.* Nutrition Reviews, 2007. **65**(3): p. 122-129.
73. Siva, K., et al., *A Phenotypic Screening Assay Identifies Modulators of Diamond Blackfan Anemia.* Slas Discovery, 2019. **24**(3): p. 304-313.

## Figure legends

**Figure 1. Association of disruptive OXPHOS pathway with DBA pathology.**

A. Pathway enrichment analysis of DEGs in DBA samples against ITP controls showing that the OXPHOS pathway was significantly suppressed in patients with DBA. B. Heatmap analysis of key genes in OXPHOS pathway mapped to all DBA and control samples showing that the OXPHOS pathway was suppressed in 7 of 10 patients with DBA, among which DBA patient 5 (*RPL11* mutation) showed suppression of the OXPHOS pathway, whereas DBA patients 9 (*RPS19* mutation) and 10 (*RPL5* mutation) did not. C. Heatmap analysis of genes in ribosome biogenesis pathway against all DBA and control samples showing that the ribosome biogenesis pathway was also suppressed in the same batch of DBA samples (7 of 10) as in those with the suppressed OXPHOS pathway. D. GSEA analysis showing enrichment of suppressed OXPHOS and ribosome pathway in DBA samples compared to in ITP controls. E. Correlation analysis of OXPHOS and ribosome biogenesis pathway in patients with DBA. After calculating the TPM expression value of OXPHOS and ribosome pathway genes in each DBA sample, we standardized the gene expression value relative to the min-max, mapped the data to the [0,1] interval, and used the R package "ssGSEA" to analyze the OXPHOS and ribosome pathways and determine the score matrix of these two pathways in different samples. R package "corrplot" was used to calculate the correlation of the gene expression of these two pathways based on this score matrix. F. UMAP plot of single-cell cluster distribution of cells in the bone marrow from healthy individuals. This plot covers all differentiated cells towards the erythroid lineage; G. GSVA of cells at different stages of HSC differentiation into red blood cells.

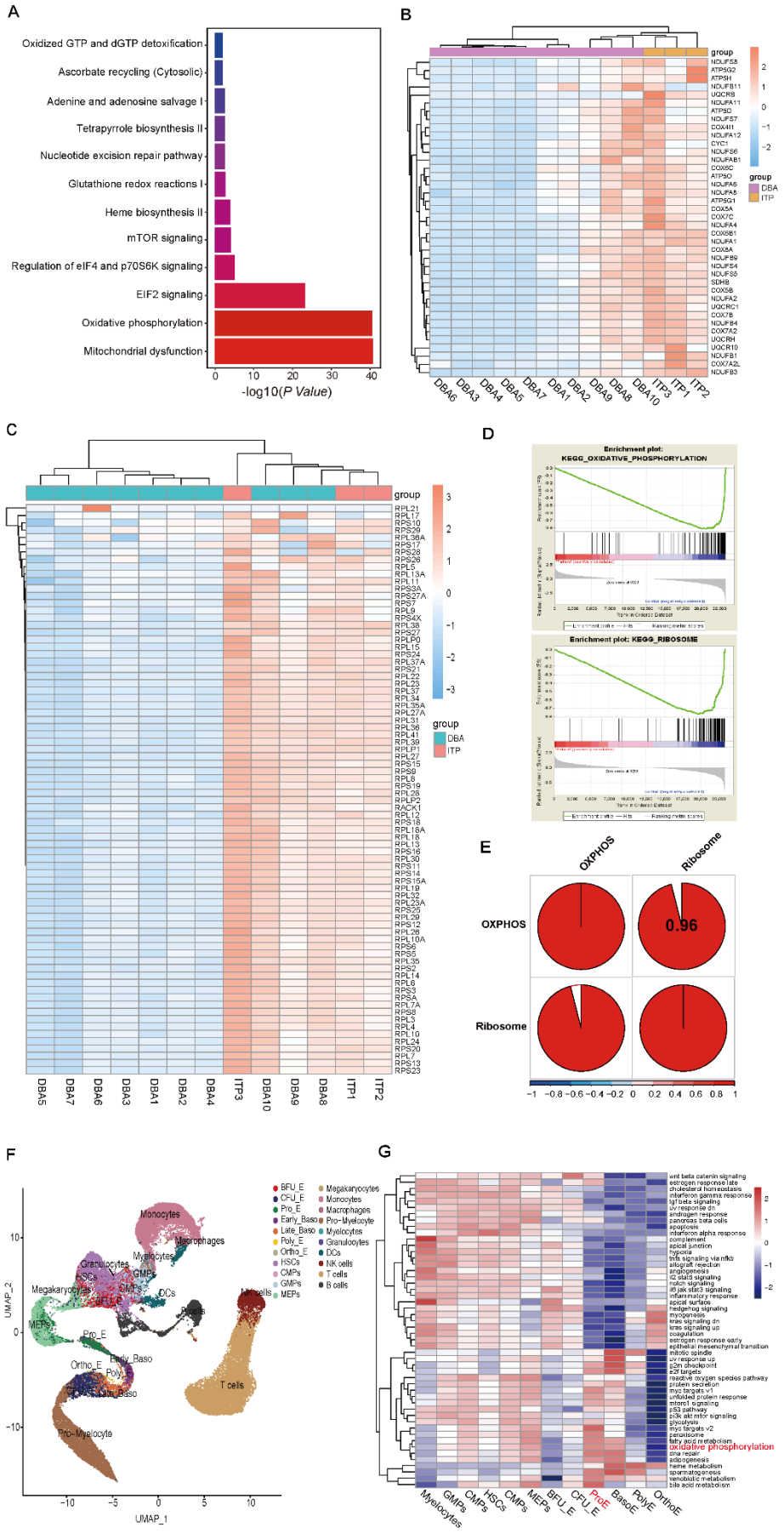
A
Oxidized GTP and dGTP detoxification
Ascorbate recycling (Cytosolic)
Adenine and adenosine salvage I
Tetrapyrrole biosynthesis II
Nucleotide excision repair pathway
Glutathione redox reactions I
Heme biosynthesis II
mTOR signaling
Regulation of eIF4 and p70S6K signaling
EIF2 signaling
Oxidative phosphorylation
Mitochondrial dysfunction
0 10 20 30 40
-log10(P Value)
B
group
DBA
ITP
DBA6 DBA3 DBA4 DBA5 DBA7 DBA1 DBA2 DBA9 DBA8 DBA10 ITP3 ITP1 ITP2
C
group
DBA
ITP
DBA5 DBA7 DBA6 DBA3 DBA1 DBA2 DBA4 ITP3 DBA10 DBA9 DBA8 ITP1 ITP2
D
Enrichment plot: KEGG_OXIDATIVE_PHOSPHORYLATION
Enrichment plot: KEGG_RIBOSOME
E
OXPHOS
Ribosome
0.96
F
BFU_E
CFU_E
Pro_E
Early_Baso
Late_Baso
Poly_E
Ortho_E
HSCs
CMPs
GMPs
MEPs
Megakaryocytes
Monocytes
Macrophages
Pro-Myelocyte
Myelocytes
Granulocytes
DCs
NK cells
T cells
B cells
UMAP_1
UMAP_2
G
Myelocytes GMPs CMPs HSCs CMPs MEPs BFU_E CFU_E ProE BasoE PolyE OrthoE
oxidative phosphorylation

**Figure 2. Suppression of OXPHOS specifically leads to failure of erythroid progenitor differentiation**

A–B. Flow cytometry analysis of Rot-treated HSPCs cells showing inhibition of OXPHOS pathway by Rot in dose- and time-dependent manners, respectively. C. Colony-forming potential analysis of Rot-treated HSPCs showing specific erythroid defects that were not observed in other lineages. D. Flow cytometry analysis showing a significantly reduced number of CD71+GlyA+ double-positive erythroid cells differentiated from Rot-treated HSPCs compared with control cells. E–F. Flow cytometry analysis showing severe blockage at the stage of erythroid progenitors (CD34+CD36+) derived from Rot-treated HSPCs in healthy BM and cord blood in differentiating DBA cells on day 7. G–I. Real-time PCR analysis showing a dramatic decrease in the expression of erythroid-specific globin genes (*HBG*, *HBB*), heme biogenesis-related genes, and other erythroid-specific genes including TFs in DBA cells on day 7. *ACTIN* was used as reference gene in real-time PCR assays. Student's *t*-test was used in this study: *$p < 0.05$; **$p < 0.01$; ***$p < 0.001$.

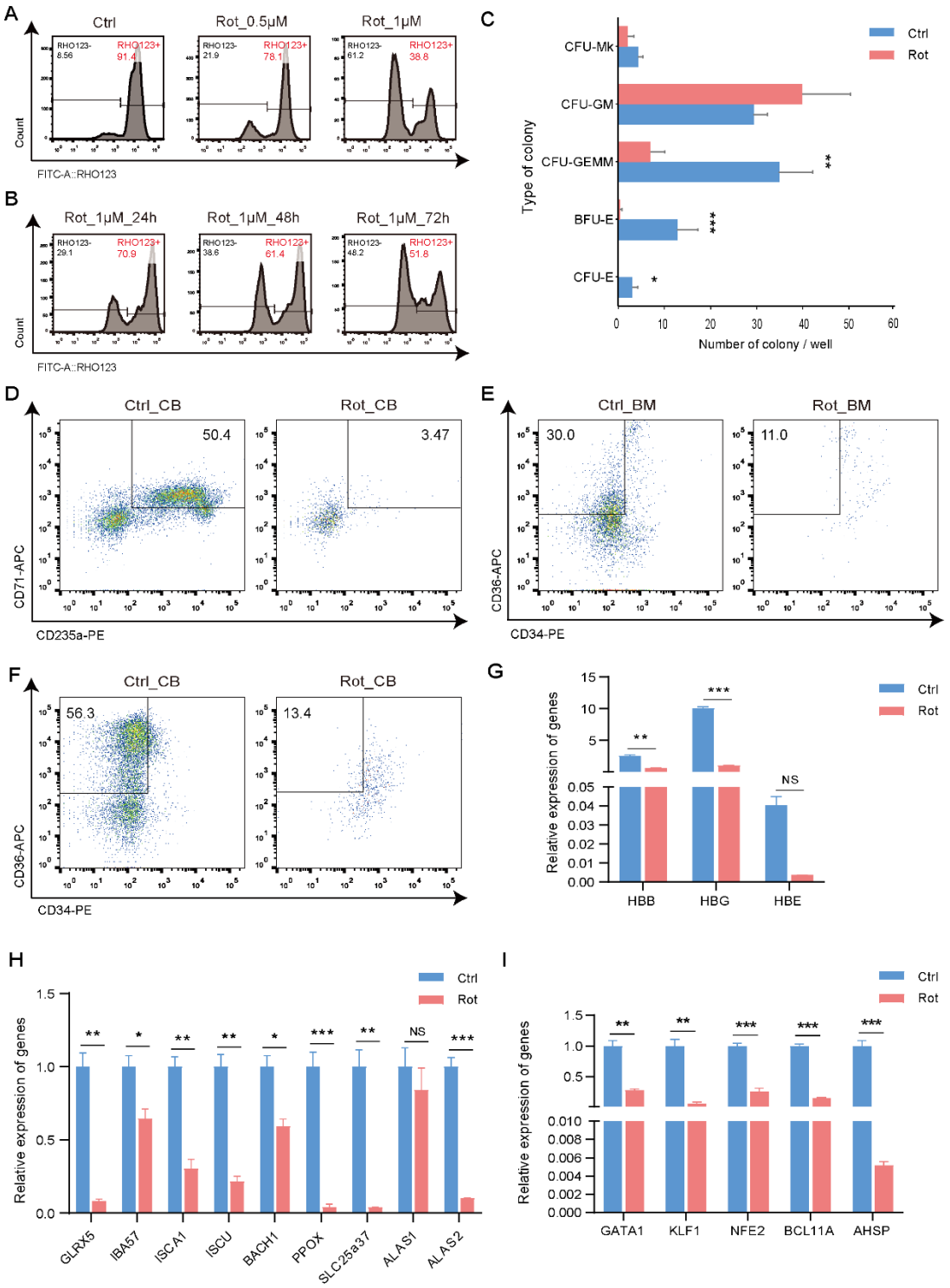


**Figure 3. Suppression of OXPHOS leads to ribosomal defects**

A. Schematic of transcriptome analysis of DBA cells during erythroid differentiation to explore the effects of inhibition of OXPHOS. Differentiating cells on days 3 and 7

treated with Rot were collected and evaluated using bulk transcriptome sequencing. The differentiated cells on days 3 and 7 respectively represent most erythroid progenitors and earlier stage erythroblasts (e.g., Pro-E, Baso-E) during erythroid differentiation of HSPCs. B. Enrichment analysis of GO terms enriched by up- and downregulated DEGs in DBA samples as well as differentiating cells on days 3 and 7, respectively. C. Real-time PCR analysis showing significantly overall reduction in the expression of most DBA causative genes identified in differentiating DBA cells on day 7. *ACTIN* was used as the reference gene. D. Real-time PCR analysis showing decreased expression of *RPS6* in differentiating DBA cells on day 7. *ACTIN* was used as a reference gene. ***$p < 0.001$. E. Immunofluorescence analysis for RPS6 showing the defects in ribosome in differentiating DBA cells on day 7.

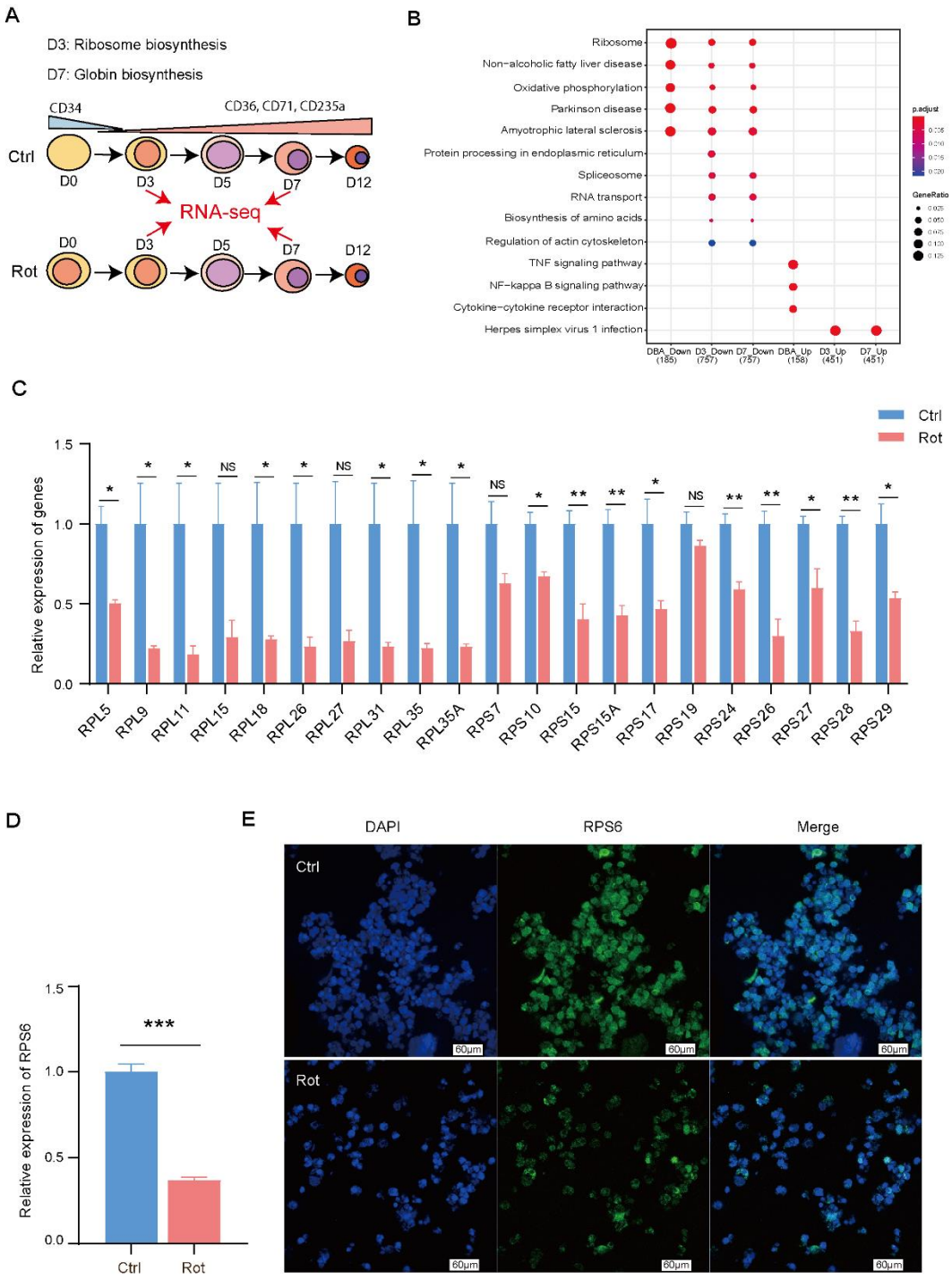


**Figure 4. Knockdown of RanGAP1 leads to erythroid defects**

A. Mapping analysis showing downregulation of RNA-transport pathway in patients with DBA and in DBA cells on days 3 and 7. The arrow indicates the suppressed RAN

protein which plays a key role in RNA nuclear transport and can be activated by RanGAP1. B. Western blotting assay showing the abolishment of RanGAP1 protein expression in DBA cells on day 7. The expression of SUMO1/RanGAP1 complex was simultaneously detected using the RanGAP1 antibody. Actin was used as a loading control. C. Real-time PCR analysis showing the knockdown of RanGAP1 by two independent shRNAs targeting different coding regions in RanGAP1 on day 7. ***$p < 0.001$. D. Western blotting assay confirmed knockdown of RanGAP1 with shRNAs in differentiated erythroid cells from cord blood HSPCs on day 7. The expression of HBG protein was decreased in differentiated cells with RanGAP1 knockdown. GAPDH was used as a loading control. E. RanGAP1 knockdown delays erythroid differentiation as revealed by the color of the cell pellets on day 7. Differentiated cells containing the control vector appeared as a red pellet, whereas pelleted cells with RanGAP1 knockdown did not; E. Flow cytometry analysis showing decreased number of CD71+GlyA+ double-positive erythroid cells differentiated from cord blood HSPCs with RanGAP1 inhibition on day 7.

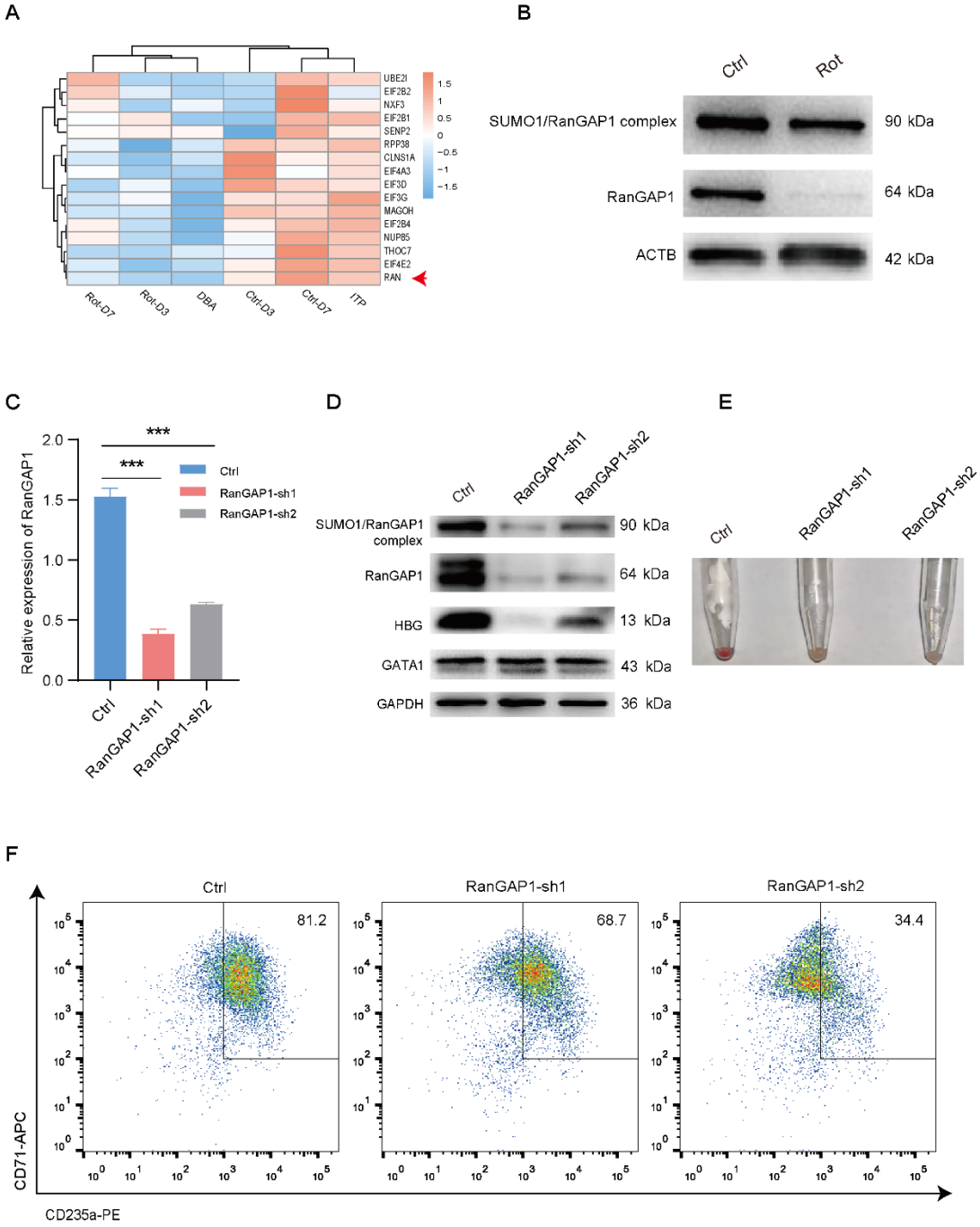


**Figure 5. Integrative analysis showing both erythroid defects and ribosomal abnormality in DBA cells**

A. Schematic of integrative analysis of proteome and transcriptome sequencing data in DBA cells. The differentiated cells on day 7 with or without Rot treatment were

simultaneously subjected to TMT mass spectrometry and bulk transcriptome sequencing. Three biological replicates were evaluated for each treatment. B. Heatmap analysis showing the overall reduction of all ribosome constituted proteins at both the protein and mRNA levels. C. Heatmap analysis showing erythroid defects revealed by decreased expression of erythroid-specific proteins at both the protein and mRNA levels, including erythroid markers, transcription factors, hemoglobin, and heme biosynthesis pathway-related components. D. Functional enrichment of simultaneously differentially expressed genes and proteins in DBA cells. The figure was constructed using ClusterProfiler. E. Identified proteins without changes in transcript expression but with significant decreases in protein expression. The translation of these proteins may be affected by ribosome disorder resulting from inhibition of the OXPHOS pathway. The functions of most listed proteins in erythropoiesis are largely unknown. F. Functional enrichment analysis of significantly downregulated proteins without changes in transcript levels in DBA cells showing disturbed pathways. The figure was constructed using ClusterProfiler.

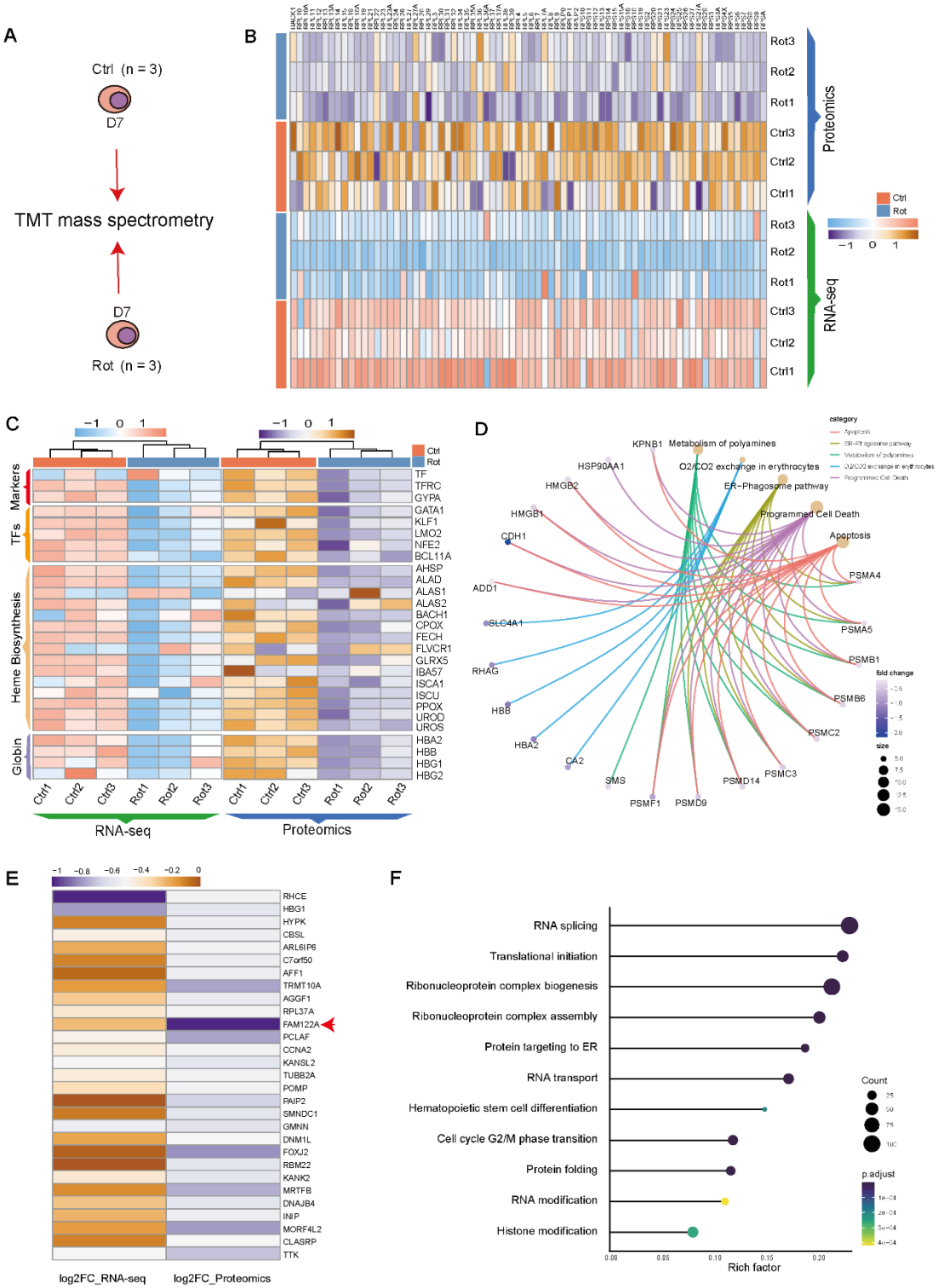


**Figure 6. CoQ10 alleviates erythroid defects in DBA cells**

A. Flow cytometry analysis showing CoQ10 largely recovered the inhibition of OXPHOS caused by Rot treatment in DBA cells. B. ATP level was largely rescued by

CoQ10 following Rot treatment in DBA cells. *$p < 0.05$; ***$p < 0.001$. C. Expression of RanGAP1 in DBA cells was largely rescued with addition of CoQ10 to differentiating DBA cells on day 7. Expression of the SUMO1/RanGAP1 complex was detected using an RanGAP1 antibody. D. Flow cytometry analysis showing an increased number of CD71+GlyA+ double-positive erythroid cells following addition of CoQ10 to differentiating DBA cells on day 7. E. Giemsa staining showing that addition of CoQ10 mostly rescued erythroid defects of DBA cells. Differentiated cells were visualized on day 7.

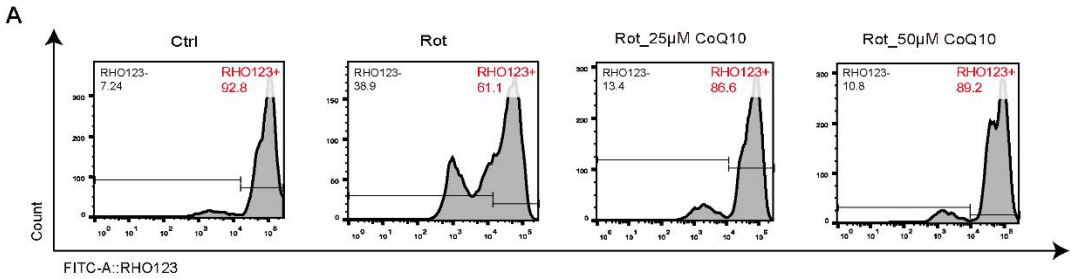
A
Ctrl
Rot
Rot_25μM CoQ10
Rot_50μM CoQ10
RHO123-
7.24
RHO123+
92.8
RHO123-
38.9
RHO123+
61.1
RHO123-
13.4
RHO123+
86.6
RHO123-
10.8
RHO123+
89.2
Count
FITC-A::RHO123

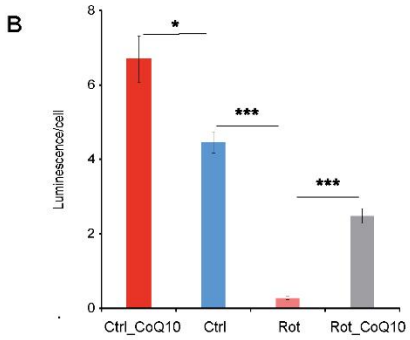
B
Luminescence/cell
*
***
***
Ctrl_CoQ10
Ctrl
Rot
Rot_CoQ10

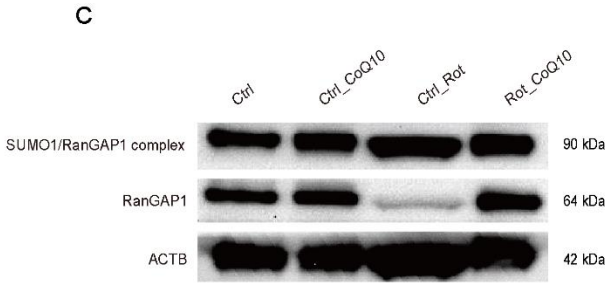
C
Ctrl
Ctrl_CoQ10
Ctrl_Rot
Rot_CoQ10
SUMO1/RanGAP1 complex
90 kDa
RanGAP1
64 kDa
ACTB
42 kDa

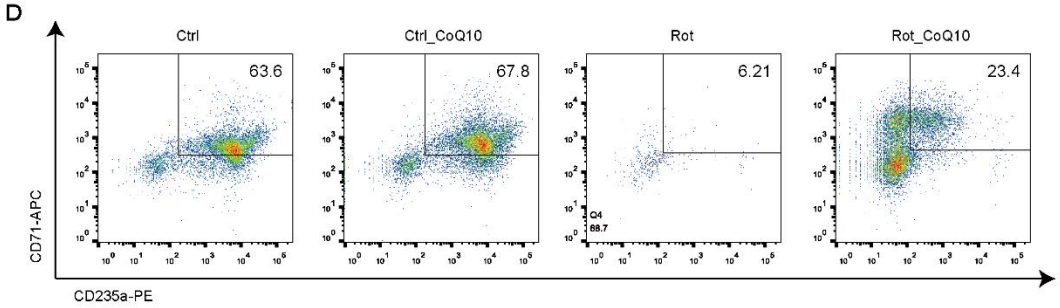
D
Ctrl
Ctrl_CoQ10
Rot
Rot_CoQ10
63.6
67.8
6.21
23.4
CD71-APC
CD235a-PE

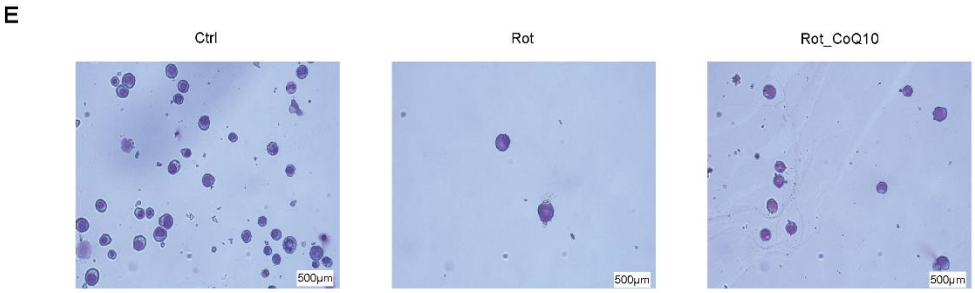
E
Ctrl
Rot
Rot_CoQ10
500μm
500μm
500μm